A Shear-Induced Martensitic-like Transformation in a Block Copolymer Melt

Catheryn L. Jackson,* Kathleen A. Barnes,† Faith A. Morrison,† Jimmy W. Mays,‡ Alan I. Nakatani, and Charles C. Han

Materials Science and Engineering Laboratory, National Institute of Standards and Technology, U.S. Department of Commerce, Gaithersburg, Maryland 20899

Received August 9, 1994; Revised Manuscript Received October 25, 1994®

ABSTRACT: The coexistence of two cylindrical microstructures of different symmetries has been observed in a sheared and quenched poly(styrene-d_8)/polybutadiene/poly(styrene-d_8) (SBS) block copolymer (23 wt % styrene-d_8) by small-angle neutron scattering and transmission electron microscopy. Near the order–disorder transition (ODT) temperature, the equilibrium cylindrical microstructure with $d_{(100)} = 21 \pm 2$ nm and cylinder diameter of about 12 nm orients in the shear field as expected based on previous reports. Above a critical shear rate and at an appropriate strain, a new shear-induced cylindrical microstructure forms. The shear-induced structure consists of grains of cylinders with a smaller diameter (8–9 nm) and a $d_{(110)}$ spacing of 12 nm. The transformation which occurs, from the original $p31m$ space group with a unit cell dimension $a = 25$ nm to a $p3m1$ space group of lower symmetry, also with $a = 25$ nm, is analogous to martensitic transformations which occur in metals during deformation processes. This transformation may be a result of the preferred orientation of the original cylindrical microstructure relative to the shear field and the imposition of a nonsymmetric (simple shear) deformation.

I. Introduction

Block copolymers exhibit unique thermodynamic phases which are absent in the corresponding homopolymer blends. The bond constraint linking the polymer blocks serves to "frustrate" macroscopic phase separation, resulting in various microphase-separated morphologies. The transition from a homogeneous, disordered state to an ordered morphology (lamellae, cylinders, spheres, etc.) with the variation of temperature is referred to as either the order–disorder transition (ODT) or the microphase separation transition (MST). A variety of ordered morphologies can be obtained by varying the relative block lengths, overall composition, and other factors,[1,2] and there has been interest in testing mean-field theories for this unique transition. The role of fluctuations in this type of transition is also an active area of research which raises many theoretical and experimental issues.[3,4] The ODT is a more subtle transition than macroscopic phase separation in homopolymer blends, where thermal fluctuations of the polymer concentration exhibit themselves dramatically through a diverging correlation length and scattering intensity at the transition temperature. These singular features do not exist in the scattering data of block copolymers at the ODT since the elastic forces associated with chain connectivity suppress the thermodynamic fluctuations at long wavelengths. Viscoelastic measurements are often employed to locate the ODT temperature.

Interest in block copolymers has turned from the characterization of equilibrium properties to the properties of these fluids subject to flow.[5–14] Experiments such as these are vital for understanding the influence of shear on the structure and phase behavior or block copolymers. In addition, a knowledge of shear-induced transitions is important in controlling block copolymer morphologies under real processing conditions for these materials. In the present work, we describe small-angle neutron scattering (SANS) and transmission electron microscopy (TEM) observations which show a novel shear-induced transition in the morphology of a block copolymer melt under steady shear flow. Previous studies of the phase behavior of blends of linear polymers have revealed significant changes with shear,[15,16] and profound changes with shear are also observed for block copolymer melts. A tentative theoretical discussion of the observed transition is also presented.

There have been other reports on the effect of deformation on the morphologies of block copolymer melts. Studies of diblock[4–8] and triblock[8–14] copolymers have included extrusion through a tube,[9] steady shearing,[7,11–12,14] oscillatory shearing,[5–7,10,13] and roll-casting.[8] The main effect of shear is the orientation of lamellar[4–8] and cylindrical[8–14] phases with flow. Most of these studies have relied on quenched specimens, where the effect of the quench on the final structure is difficult to assess. More recently, in-situ SANS studies have shown an apparent increase in the isotropic-to-lamellar transition temperature in an oscillating shear field.[5] Various intermediate phases have been detected between the lamellar and cylindrical phases of a diblock copolymer upon heating and shearing through the transition region.[6] The nature of these intermediate phases is related to the necessary transformation of the lamellar morphology to a cylindrical morphology and they are termed hexagonally modulated lamellae and layered hexagonal-packed channels. The theories predicting block copolymer phase behavior[17,18] have mostly concentrated on quiescent systems, but recent theories for the effect of shear on diblock copolymers have been reported.[19,20] The added complexity of structure in triblock copolymers, which can adopt more than one equilibrium conformation, has limited the development of theories for these technically important materials.[3]

This work builds on the results from our recent collaboration[14] on the structure of a poly(styrene-d_8)/polybutadiene/poly(styrene-d_8) (SBS) block copolymer (23 wt % styrene-d_8, cylindrical morphology) in a steady shear field as studied by small-angle neutron scattering

† Department of Chemical Engineering, Michigan Technological University, Houghton, MI 49931-1295.
‡ Department of Chemistry, University of Alabama, Birmingham, Birmingham, AL 35294.
® Abstract published in *Advance ACS Abstracts,* January 15, 1995.

0024-9297/95/2228-0713$09.00/0

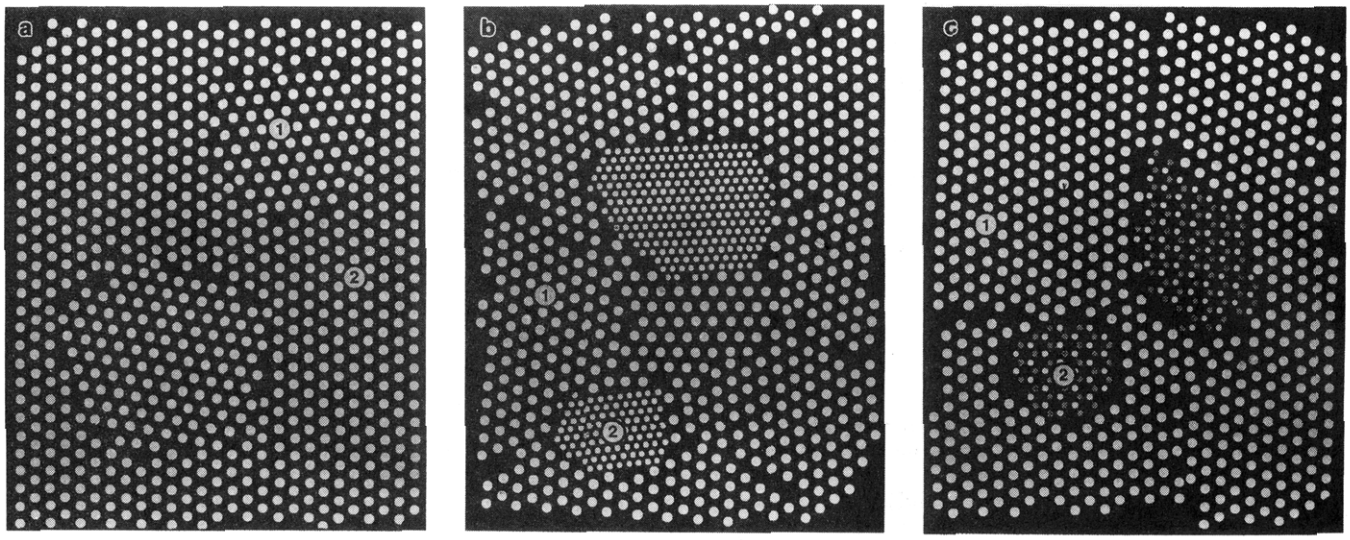

Figure 1. Schematic drawing of the proposed structures formed in shear flow in the *yz* plane where the region labeled 1 is the primary structure and the region labeled 2 is the shear-induced morphology. The white and shaded circles are PS-rich cylinders, end-on, and the black background is the matrix, or PB-rich phase. (a) Model 1, hexagonally packed PS cylinders of near-perfect order coexist with randomly oriented grains of PS cylinders. (b) Model 2, two types of grains of different unit cell parameters and different PS cylinder diameters coexist. (c) Model 3, two types of grains with the same unit cell parameters but different symmetries and different cylindrical diameters coexist.

(SANS). These in-situ measurements were made in a Couette geometry as a function of shear rate and temperature, near the apparent ODT temperature of 116 °C, as determined rheologically. At low shear rates, the scattering was anisotropic, with a set of peaks observed at low scattering angle, normal to flow. This represents an orientation of the cylinders in the flow direction, as previously reported in these systems[9-12] for quenched specimens. Above a critical shear rate, a second set of peaks appeared at a higher scattering angle. The ratio of the scattering vector values, q, for the two sets of peaks was 1:1.7 (where $q = (4\pi/\lambda)\sin(\theta/2)$, θ is the scattering angle, and λ is the incident radiation wavelength). Thus, the peak positions were consistent with reflections from the (100) and (110) planes of a hexagonally packed cylindrical array, with a unit cell parameter $a = 25$ nm. However, the time dependence of the scattering behavior after cessation of shear provided strong evidence that the two peaks originated from two distinct structures. The low-q peak was observed to broaden azimuthally and become isotropic in a short time (120 s), while the high-q peak remained sharp over the same time period. After much longer times or upon increasing the temperature, the high-q peak dissipated; thus the formation of the shear-induced structures was reversible. The high-q peak also had a different shape than the low-q peak, which is further evidence that the two peaks arose from two different structures.

Two models were suggested[14] for the structure produced at high shear rates. The essential features are shown in Figure 1. For each model, the existence of two types of grains was proposed. The first type of grain (labeled 1) is common to both models, and the second type of grain (labeled 2) is unique to each model. The first type of grain corresponds to hexagonally packed cylinders ($a = 25$ nm) with the long axis of the cylinders aligned along the x axis, or flow direction. In this case, the grains are cylindrically symmetric about the x axis and the cylinders of polystyrene are shown as the white circles (Figure 1a–c). The black background is the polybutadiene matrix. In Model 1, we hypothesized that the second grain structure consists of polystyrene cylinders in nearly perfect, hexagonally packed domains with the (110) planes oriented at a specific angle relative to the shear field, shown in Figure 1a. In Model 2, we hypothesized a second grain structure with a much smaller cylinder size and different unit cell dimensions ($a = 14.5$ nm), shown in Figure 1b. We proposed that this structure may form above a threshold shear rate and hypothesized that chains in a "bridging" configuration between cylinders may reassemble in a predominantly "looping" configuration. Both of the models were consistent with the observed features in the scattering data, and the present study seeks to resolve the possible morphologies.

In this work, we examine a sheared and quenched block copolymer using SANS and TEM. The same deuterated SBS triblock copolymer[14] is used for this study, but the samples are prepared in a cone-and-plate rheometer, under conditions similar to the SANS Couette cell. The cone-and-plate rheometer allows the specimen to be easily quenched to room temperature and removed from the fixtures. In addition, a quiescent film of the polymer was slowly cast from solution to compared the equilbium morphology to the shear-induced morphology in the TEM.

The evidence discussed below forces us to introduce a third model (Figure 1c) as the most likely shear-induced morphology. The morphology of Model 3 also corresponds to a two-grain picture and is similar to Model 2, but the symmetry of the hexagonal structure formed is distinctly different, as shown in Figure 1c. This morphological transition is analogous to a martensitic-like transformation[21] observed in metallurgical systems. This transformation is often a result of a deformation process, as in the shear measurements described in this report. The parallelism in this phenomenology gives us confidence that the assignment of our observed morphology for sheared block copolymers is reasonable.

II. Experimental Section

Materials. A poly(styrene-d_8)/polybutadiene/poly(styrene-d_8) (SBS) block copolymer with a block architecture of $8 \times 10^3/54 \times 10^3/8 \times 10^3$ g/mol ($M_w/M_n = 1.05$) was synthesized by coupling living diblock under vacuum using dichlorodimethylsilane, followed by fractionation to remove residual diblock polymer.[14] The molecular weight was analyzed after the shearing studies as well and found to be largely unchanged

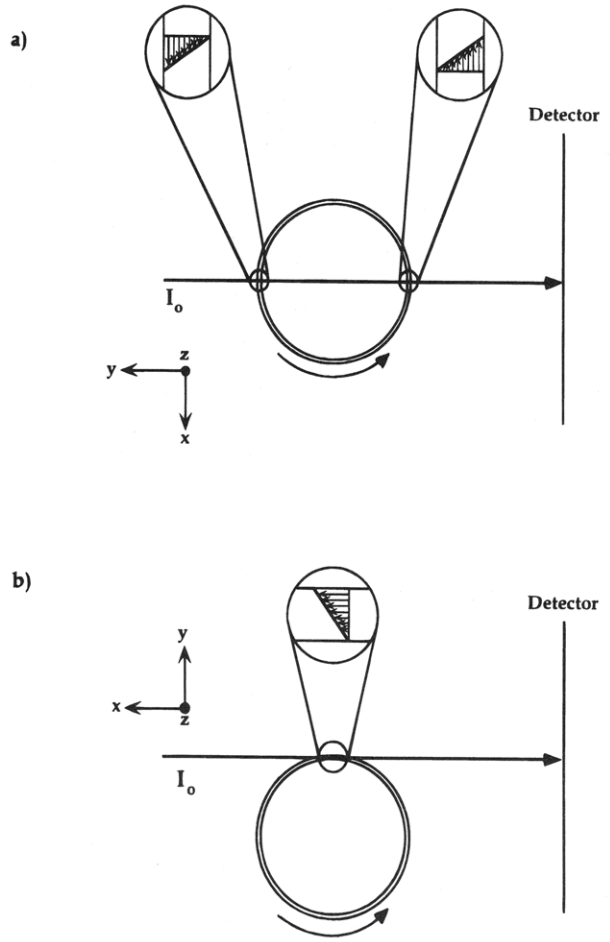

Figure 2. Schematic of the SANS Couette cell showing (a) the through-view with the detector in the *xz* plane and (b) the tangential view used to look along the flow direction with the detector in the *yz* plane.

with the exception of a small amount of higher molecular weight material. Very little formation of the precursor diblock copolymer upon shearing is observed, as measured by SEC. The overall composition of the polymer is 23 wt % polystyrene, and the ordered phase of this sample is a hexagonally packed cylindrical array. The ODT of this material was 116 ± 5 °C, by dynamic mechanical measurements. The glass transition of the polystyrene phase in this sample is estimated to be ~80 °C.[7]

A cone-and-plate Bohlin VOR[22] shear rheometer with a fixture diameter of 1.5 cm was used to prepare quenched, sheared samples for both SANS and TEM studies. The conditions used were shear rates of 0.294 and 0.585 s^{-1} at 100 °C for a series of different strains. The "quench" was done by stopping the rheometer, turning off the heater, and opening the oven to cool to ambient temperature as soon as possible. In addition, the cone-and-plate was quickly detached from the rheometer assembly to prevent the contraction of the tooling from imposing an extensional flow on the sample. Prior SANS studies indicated that below T_{ODT} the relaxation of scattering patterns from anisotropic to isotropic was quite slow (>30 min).

Small-Angle Neutron Scattering. SANS experiments were performed at the Cold Neutron Research Facility (CNRF) at the National Institute of Standards and Technology (NIST) using an incident wavelength of 0.6 nm for the in-situ melt studies. The SANS shear cell used has been described previously.[23] In the standard configuration, the shear gradient is oriented so that the incident beam is parallel to the gradient axis (*y* direction) and scattering is monitored in the *xz* plane (*x* is the flow direction and *z* is the neutral direction). We refer to this as the *xz* or through-view, as shown in Figure 2a. We have also translated the apparatus so the beam enters the Couette cell tangentially. We refer to this as the *yz* or tangential view. In this case, the beam is parallel to the flow direction, and scattering is monitored in the *yz* plane, as shown in Figure 2b.

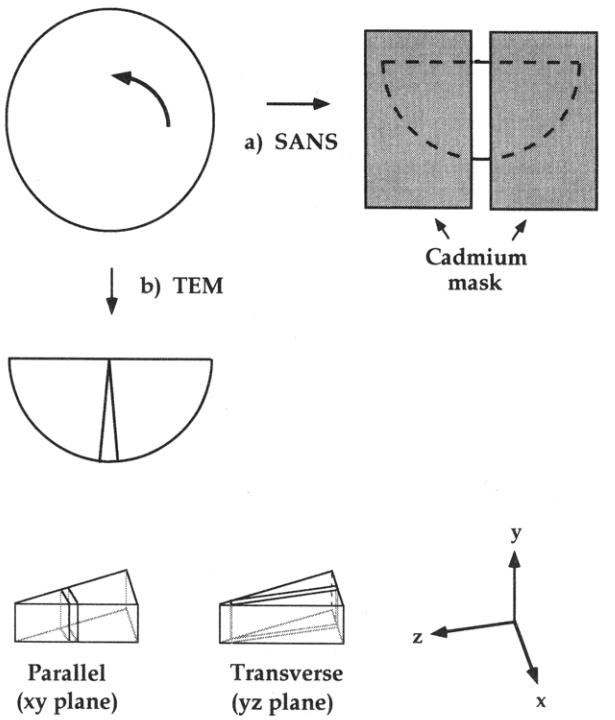

Figure 3. Schematic of the cone-and-plate disk showing the dissection of the specimen for (a) SANS and (b) ultramicrotomy and TEM studies.

SANS measurements on the quenched disks from the cone-and-plate rheometer were run using a vertical cadmium mask on a half-disk of the sample so that only a slit-shaped region was illuminated, as illustrated in Figure 3a. This represents the *xz* plane, or shear plane, in the cone-and-plate geometry, with the beam normal to this plane. This view is equivalent to the through-view for the in-situ studies, shown in Figure 2a. For this experiment, a slightly longer wavelength of 0.9 nm was used compared to our earlier results (ref 14, $\lambda = 0.6$ nm). SANS results reported for the quenched sample have not been corrected for background scattering and are not scaled to absolute intensity. The measurements were performed solely for verifying the existence of the second set of scattering peaks; therefore these corrections were not necessary.

Ultramicrotomy and Electron Microscopy. The quenched disks were dissected for TEM studies as illustrated schematically in Figure 3b. The sections were cut such that the surface normals were parallel and perpendicular (transverse) to the flow direction, *x*. The parallel view is cut with the knife edge perpendicular to the *z* axis (the *xy* plane) and the transverse view is cut with the knife edge perpendicular to the *x* axis (the *yz* plane). Ultrathin sections were cryomicrotomed at −100 °C and transferred dry to carbon-coated Cu grids of 200 mesh. The nominal section thickness was 50−70 nm. The polybutadiene blocks were selectively stained with osmium tetraoxide vapors after sectioning by exposing the grid to vapor from a 4% aqueous solution at room temperature for 4 h. A Philips 400T[22] model TEM was used at 120 kV to obtain the images. Low-dose EM techniques were employed, including use of a small condenser aperture (20 μm), small spot size, and reduced beam current, to preserve specimen integrity.

A quiescent film (~0.5 mm thick) of the polymer was cast from a 5% solution in toluene by evaporating the solvent slowly over a 5 week period. Toluene is a good solvent for both polystyrene and polybutadiene.[24] The film was cut and stained as described above for the sheared samples.

The negatives from the TEM were examined on an optical bench equipped with a He/Ne laser ($\lambda = 632.8$ nm) and calibrated with the image of a diffraction grating. The optical diffractograms were recorded on Polaroid Type 55 (ASA 50) film and used to measure the observed spacings on the negative.

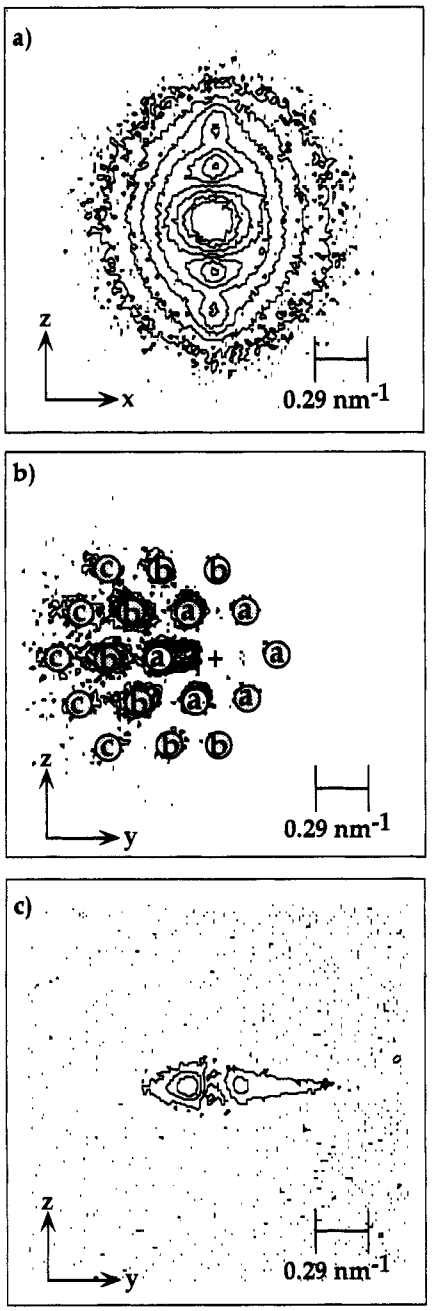

Figure 4. In-situ 2-D SANS intensity contour plots for scattering in the Couette shear cell at 110 °C and 1.3 s^{-1} for the (a) through-view or *xz* plane (counting time, 120 s) and (b) tangential view or *yz* plane (counting time, 120 min). (c) Empty cell scattering for tangential view.

III. Results

SANS. The effect of shear on the SANS behavior of a SBS block copolymer in the melt is shown in Figures 4a and 4b for the two views outlined schematically in Figures 2a and 2b, respectively. The shear rate used in this case was 1.3 s^{-1} at a temperature of 110 °C, which is below the T_{ODT} of 116 °C. These conditions are sufficient to produce the dual peaks in the scattering for the through-view, as shown in Figure 4a and described in a prior communication.[14] The low-q peak ($q_{max1} = 0.29 \pm 0.01$ nm^{-1}, $\theta = 2.4 \pm 0.1°$, $d_{(100)} = (2\pi/q) = 21.7$ nm) corresponds to the spacing expected for the equilibrium structure while the higher q peak ($q_{max2} = 0.50 \pm 0.01$ nm^{-1}, $\theta = 4.1 \pm 0.1°$, $d_{q_{max2}} = 12.5$ nm) is believed to be due to the shear-induced structure.

To confirm that orientation of the cylinders in flow is occurring, the tangential geometry (Figure 2b) was utilized with the result shown in Figure 4b. When positioning the shear cell in this way, strong reflections from the empty Couette cell appear, as shown in Figure 4c. The beam stop is denoted by the (+) in the center of the detector field of Figure 4b. In addition, a somewhat skewed pattern is observed due to the curved sample volume. Only half of the detector is seen because the scattered neutrons are not transmitted through the copper block of the stator. Relatively long times (60 min) are required for the data acquisition compared to the through-view (20–300 s), since a smaller volume is sampled in this geometry. Even with these limitations, the data in Figure 4b show that a single-crystal-like, hexagonal scattering pattern is obtained at 1.3 s^{-1} and 110 °C (counting time = 120 min). The data obtained in the tangential configuration confirm the presence of the hexagonal phase of the cylinders, aligned along the flow direction. The peaks observed are grouped as a, b, and c, respectively. The orientation of the hexagonal scattering pattern implies that the primary structure prefers the (100) planes to be nearly parallel to the *xz* plane (the shear plane) in a flow field. The weak reflection labeled c is seen in the tangential-view but not in the through-view case, presumably due to the long time scale of the experiment, 120 min, compared to that used in the through-view case (20–300 s) and the resulting perfection in orientation of the specimen.

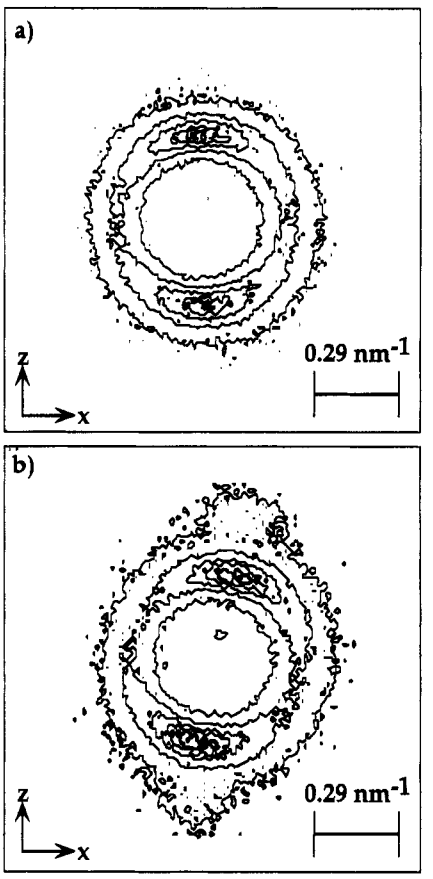

Figure 5. 2-D SANS intensity contour plots of the cone-and-plate specimens sheared at (a) 0.294 s^{-1}, 100 °C and (b) 0.585 s^{-1}, 100 °C and quenched to room temperature. The scattering shown is in the *xz* plane.

The SANS of the two quenched specimens are shown in Figures 5a and 5b for samples sheared at 0.294 and 0.585 s^{-1}, respectively, at 100 °C. At the lower shear rate of 0.294 s^{-1} (Figure 5a), a single scattering peak is observed, whereas at the higher shear rate of 0.585 s^{-1} (Figure 5b), two peaks are observed. In the original

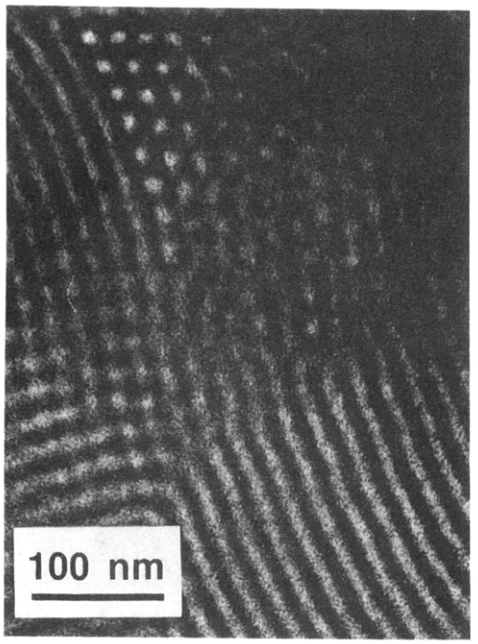

Figure 6. Transmission electron microscopy (TEM) micrograph of the quiescent film of SBS. The polybutadiene matrix has been stained dark with osmium tetraoxide, as seen in all subsequent images.

Couette experiment, both sets of conditions produced two SANS maxima,[14] and it is clear that the Couette conditions do not translate directly to the cone-and-plate. This may be caused by a combination of geometry differences and the effect of quenching. We believe, however, that the weak, high-q peak observed in Figure 5b corresponds to the shear-induced morphology observed in the in-situ SANS studies. This shear-induced morphology is a nonequilibrium structure and is difficult to capture by quenching. In both cases, the anisotropy indicates the cylinders are oriented along the flow direction. However, due to the cessation of shear and the time necessary for cooling, the quenched specimen has lost some degree of orientation. This is evident in the azimuthal broadening of the low-q peaks in Figures 5a and 5b compared to Figure 4a. The weaker, more diffuse high-q peak in Figure 5b compared to the sharp, high-q peak in Figure 4a is further evidence that the quenched sample has a lower degree of orientation than the in-situ sample.

TEM. The morphology of a quiescent film of this polymer is presented to illustrate the differences in structure between sheared and unsheared specimens. A typical example of the morphology as seen by TEM for the unsheared block copolymer as cast from toluene solution is shown in Figure 6. The polystyrene cylinders appear white while the continuous phase of the polybutadiene blocks is stained dark by osmium tetraoxide. The order structure is determined to be a hexagonally packed array of cylinders, with an approximate spacing $d_{(100)} = 20.4 \pm 3$ nm. The calculated equilibrium spacing for this polymer is $d_{(100)} = 21.7$ nm, and the cylinder diameter is approximately 12 nm. The slightly smaller spacing seen in the quiescent film is typical of cast films.[25] For example, annealing a lamellar polymer above T_g has been shown to increase the lamellar spacing by about 10% when compared to the as-cast film.[25] A small variation in spacing in differently oriented domains is observed in the as-cast films due to tilt effects. The expected reduction in spacing due to tilt of the differently oriented domains[26] is calculated to be ~3 nm, and this degree of variation is seen in different regions of the sample. No spacing smaller than 17 nm was observed after investigating many regions. The quiescent film shows no preferential orientation of cylinders, and the interface between the polystyrene cylinders and polybutadiene matrix is fairly well defined.

The morphology of the sheared, quenched block copolymer (0.294 s^{-1}, 100 °C) in the parallel view (Figure 3b) is shown in Figure 7. From this view, the structure in Figure 7 could be identified as either cylindrical or lamellar, so the transverse view is shown in Figure 8. The ordered structure is determined from both Figures 7 and 8 to be a hexagonally packed array of cylinders with an approximate spacing $d_{(100)} = 21 \pm 2$ nm from the optical diffraction pattern shown in the inset of Figure 7. The cylinder diameters are somewhat difficult to measure from the image, but they are close to the expected value of 12 nm. The cylinders and matrix have an undulating interface, which we attribute to the effect of shear on the morphology, as previously reported by others.[5,13,26] After extensive investigation of many regions, the only ordered structure found in this specimen was cylinders of this size and spacing. In this specimen, large domains of oriented cylinders were difficult to find, which corroborates the neutron scattering results discussed previously (Figure 5a).

The morphology of the sheared, quenched block copolymer made at a higher shear rate (0.585 s^{-1}, 100 °C) in the parallel condition (Figure 3b) is shown in Figure 9. The grain sizes observed in the sheared samples were, in general, smaller than observed in the quiescent film. The primary spacing seen in Figure 9 is labeled 1 and is measured to be 21 ± 2 nm. A secondary structure is also evident in Figure 9, labeled 2. This structure has a much smaller spacing of 12 ± 2 nm, and the overall fraction of this morphology present in the sample is low. The two spacings are also evident in the optical diffractogram in the inset, which illustrates that they are oriented in the same direction. It is not possible that the smaller spacing is the (110) spacing of the primary structure in this type of cylindrical block copolymer, because the diameter of the cylinders is very large ($d = 12$ nm) within the unit cell. The large errors on the d spacings reflect the approximate nature of the TEM measurement, especially since the cylinders and matrix have an undulating interface due to the shear.[26,27]

The image in Figure 9 was chosen to demonstrate the presence of both structures in the same field of view. Quantitative estimates of the amount of each structure present in the sample should not be made from the area shown, since the image may not be representative of the whole sample. The domain sizes shown also may not reflect the average domain size. For example, the region of smaller spacing labeled 2 in the upper half of Figure 9 is much smaller than another such region shown in Figure 10. A small region of the larger spacing, labeled 1, is evident in the extreme right of Figure 10, for comparison. In most areas of the sample, the large structure was predominant, and in general, the structure of small spacing was the minority component. A significant portion of poorly ordered material was also present in both of the sheared samples, which is not shown in detail here.

The morphology of the sheared, quenched block copolymer (0.585 s^{-1}, 100 °C) in the transverse view (Figure 3b) is shown in Figure 11. This confirms that the primary structure is a hexagonally packed array of cylinders, with an approximate spacing $d_{(100)} = 22 \pm 2$ nm. Based on the SANS results in Figure 4b, we have

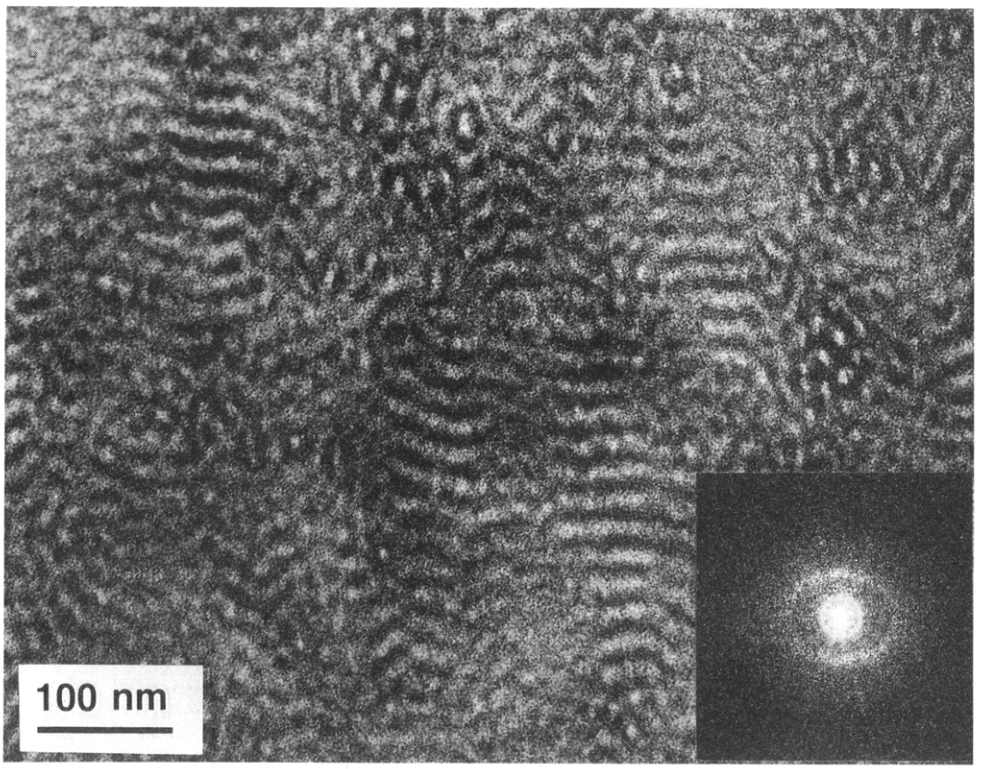

Figure 7. TEM micrograph showing morphology of the quenched, sheared SBS (0.294 s^{-1}, 100 °C), parallel view (*xz* plane, flow direction approximately horizontal). The image shows oriented domains with a spacing of ~22 nm. The optical diffraction pattern is inset.

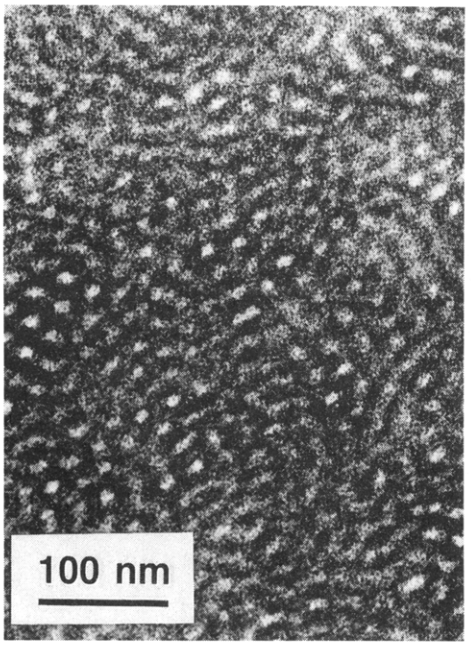

Figure 8. TEM micrograph showing morphology of the quenched, sheared SBS (0.294 s^{-1}, 100 °C), transverse view (*yz* plane, flow direction is normal to the view). Small regions of hexagonally packed cylinders with a spacing of ~22 nm are observed, along with a large amount of unoriented material.

shown the cylinders to be oriented with the (100) planes parallel to the shear plane, or *xz* plane. Another region is shown in Figure 12 where the best image of small cylinders, end-on, is identified with an arrow. The cylinder diameters are approximately 8–9 nm, which is significantly smaller than seen in the primary structure. They are fairly well resolved in a small region. The central domain of each hexagonal unit cell is absent for the region identified, and the relative intensity of the spots in the small hexagon alternate in brightness, appearing as either white or gray. This is an indication that the PS concentration in the gray cylinders is slightly lower than in the white cylinders. The small cylinders are very difficult to image due to their small diameter (~8–9 nm) relative to the sample thickness of 50–70 nm and the low volume fraction of this component. Any tilt of such a small structure would result in a poor image.

After careful consideration, we propose that the shear-induced morphology may be related to the original hexagonal microstructure as a "superlattice", with analogy to other crystalline materials. The unit cells and corresponding lattice structures are shown in Figure 13, where the positions of the cylinders in the unit cells correspond to the atomic positions in a crystallographic lattice and the two lattices are drawn to scale relative to each other. In block copolymers, the crystals are two-dimensional since the cylinders extend along the *c* axis. The unit cell of the structure in Figure 13a has the same symmetry as the $p31m$ crystallographic space group, while the unit cell of the structure in Figure 13b belongs to the $p3m1$ space group.[28] The white circles represent the PS cylinders, while the shaded circles in the $p3m1$ structure represent cylinders of some intermediate composition. This corresponds to the alternating pattern of white and gray cylinders observed experimentally in Figure 12. The dark matrix is the PB-rich phase. The reflection observed at high q is identified as the (110) spacing, $d_{(110)} \sim 12$ nm, from Figure 13b and is oriented with the (110) planes at approximately 30° to the (100) planes of the primary structure. Thus, the crystallographic spacing of the shear-induced phase is directly related to the original unit cell of the quiescent phase by $\sqrt{3}$ for the symmetry reasons outlined in Figure 13.

Although there is some uncertainty in size measurements made by TEM, we have found fairly good agree-

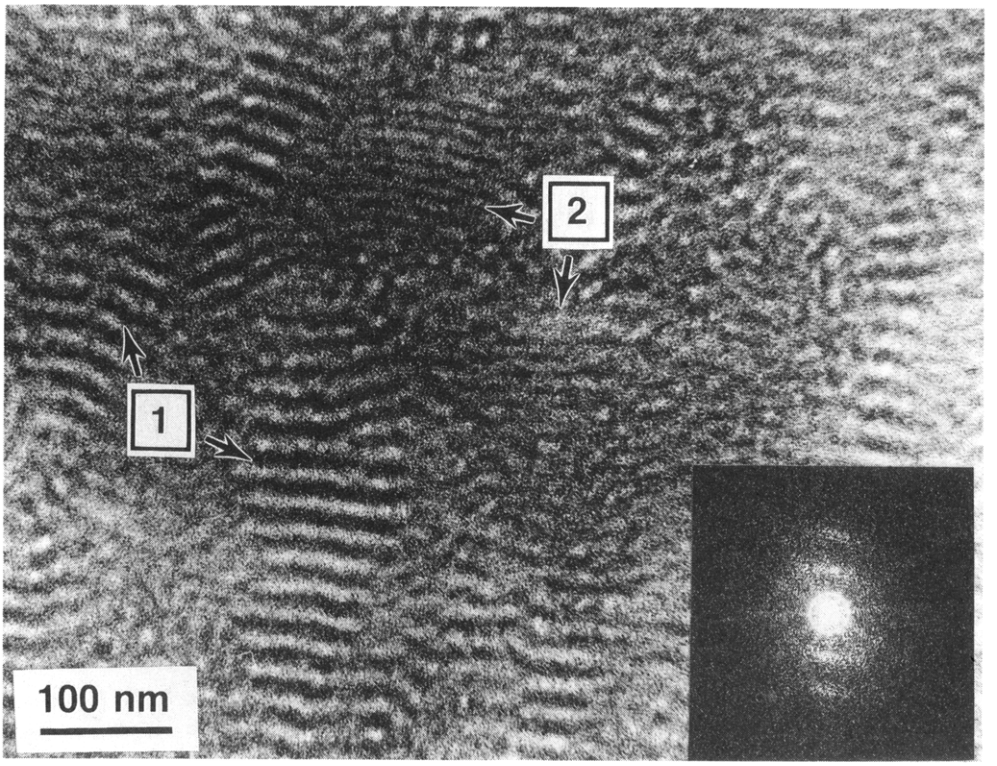

Figure 9. TEM micrograph showing morphology of the quenched, sheared SBS (0.585 s^{-1}, 100 °C), parallel view (*xz* plane, flow direction approximately horizontal). The image shows regions of large spacing (~22 nm), labeled 1, coexisting with regions of the small spacing (~12 nm), labeled 2. The optical diffraction pattern showing the two spacings is inset.

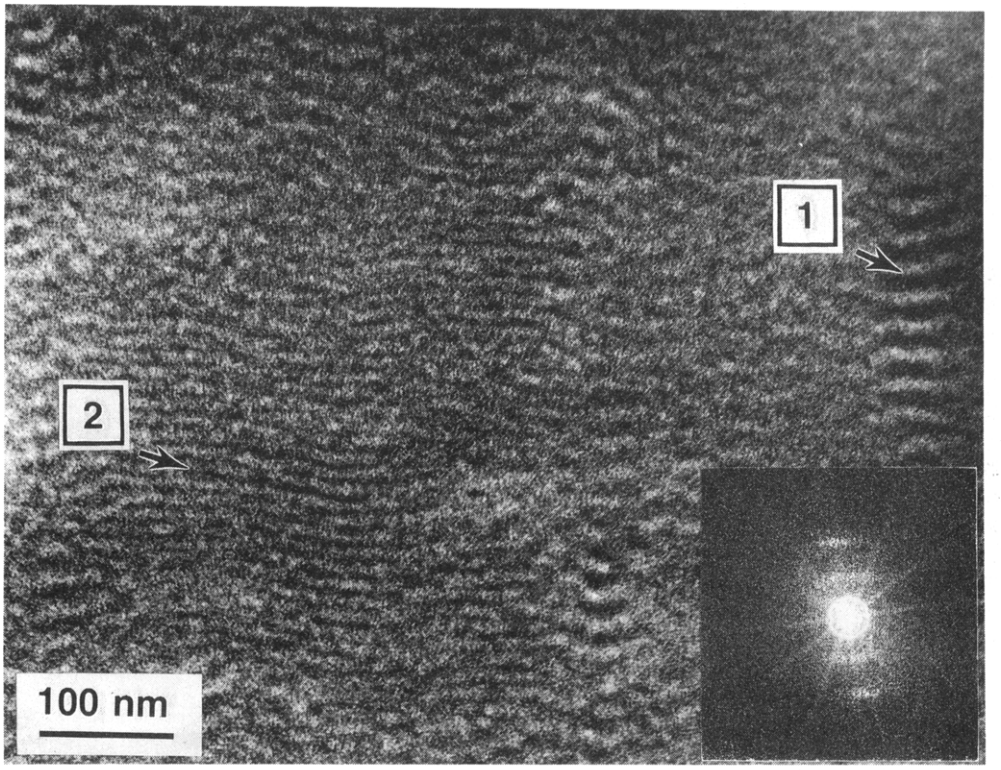

Figure 10. TEM micrograph of the same specimen and view as Figure 9, showing another region with a much larger grain of the structure with small spacing, labeled 2, coexisting with the region of large spacing, labeled 1. The optical diffraction pattern is inset.

ment between the measurements in the parallel and transverse cases. The appearance of both structures in the same field of view for both geometries directly demonstrates the relative size difference in the two structures. To our knowledge, this is the first direct TEM image of an entirely new morphology induced by shear in a block copolymer.

A discussion of possible artifacts identified by others in studies of the morphology of block copolymers by TEM,[26,29-31] including deformation during cutting, tilt effects, thickness, staining, and focusing, is relevant. Differences in the microtoming direction have been shown to cause deformation in lamellar structures, with the lamellae perpendicular to the cutting direction

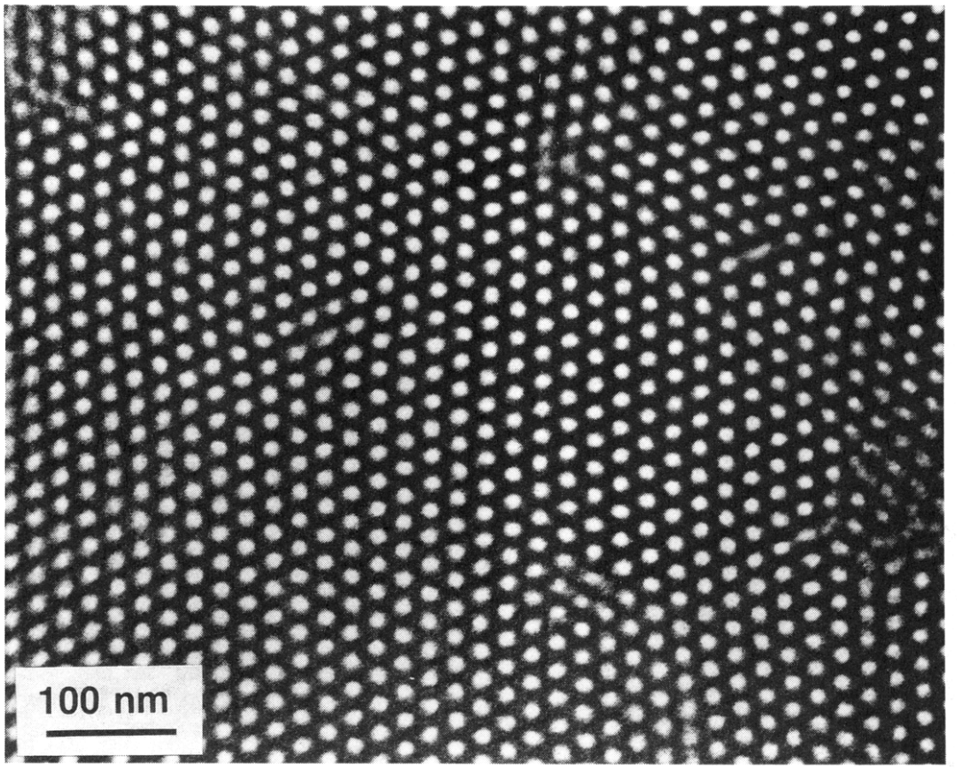

Figure 11. TEM micrograph showing morphology of the quenched, sheared SBS (0.585 s^{-1}, 100 °C), transverse view (*yz* plane, flow direction is normal to the view). Domains of hexagonally packed cylinders of large spacing (~22 nm) are the primary structure.

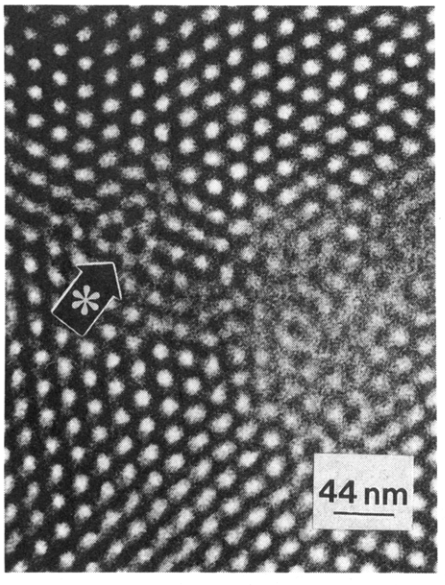

Figure 12. TEM micrograph of the same specimen as shown in Figure 11, showing another region which includes a view of the small cylinders end-on, as designated by the arrow. See text for discussion.

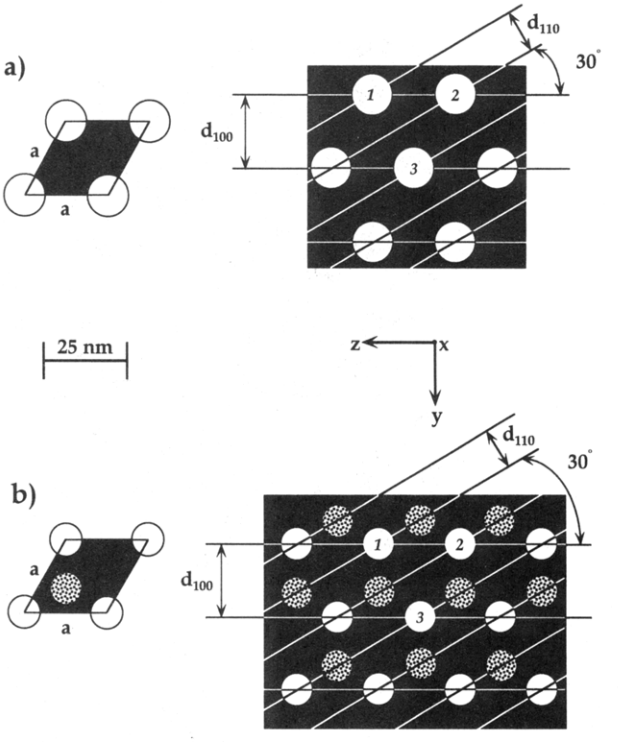

Figure 13. Hexagonal lattice projected along the *c* axis. (a) *p*31*m* space group and related "triangular hexagonal" structure. (b) *p*3*m*1 space group and related "simple hexagonal" structure, where the white circles represent cylinders of PS, the shaded circle represents an intermediate concentration of PS, and the black area is the polybutadiene matrix.

having smaller spacings than those parallel to the cutting direction.[29] This is a large effect for samples with polystyrene as the matrix and a smaller effect for samples with polybutadiene as the matrix. This effect cannot cause the difference in spacings seen in Figures 9 and 10, however, because the two structures are roughly oriented in the same direction. The tilt of the sample has also been demonstrated to produce differences in spacings for oriented cylinders in the parallel view,[26] if the samples are sufficiently thin (30–50 nm) so that only one or two layers of cylinders are in cross-section. When tilted about the rod axis, the observed diameter of the cylinders remains unaltered, while the overall center-to-center distance is reduced corresponding to the foreshortening appropriate to the degree of tilt. For hexagonally packed rods, the maximum amount of tilt is 30° due to the packing symmetry. For the sample studied here, the large spacing is 22 nm, and the maximum amount of tilt would reduce the observed

periodicity to 19 nm.[26] This is still much larger than the observed spacing in the secondary structure (12 nm) seen in Figures 9 and 10. Therefore, the secondary structure is not an artifact due to tilting of the differently oriented domains within the sample. We have considered another possible explanation for the end-on view of the small cylinders, shown in Figure 12, which appear at first glance to resemble dark regions on a bright background compared to the primary structure. Dlugosz et al.[30] also reported seeing "contrast inversion" in small regions of an oriented triblock copolymer in the transverse view and hypothesized that it was the result of a faulted region in the alignment of the cylinders. This seems unlikely for the result shown in Figure 12, in light of the images in the parallel view shown in Figures 9 and 10, but must be considered. Lastly, because the two morphologies are present in the same field of view, the relative differences in size are easy to compare directly and other minor variations in thickness, staining,[29] and focus conditions[29,31] would only change the absolute value of the measured spacings.

The possibility of molecular weight degradation of the triblock copolymer with shear, and in particular chain scisson at the center of the chain, has been considered as a mechanism for the formation of the shear-induced structure. A diblock of half the molecular weight of a triblock should form a cylindrical structure with the same spacing as the original triblock,[17] however, so molecular weight degradation would not cause the observed phenomenon. Even if some low molecular weight diluents were formed, this effect is only important if a very large amount of a second material is present (>30%) and macrophase separation occurs.[32,33] At concentrations lower than 30%, the block copolymers are mixed on a molecular level, and the observed equilibrium spacing of the higher molecular weight block copolymer is gradually reduced as it becomes diluted with lower molecular weight material.

IV. Discussion

We have observed two cylindrical microstructures having different symmetries to be present in a poly(styrene-d_8)/polybutadiene/poly(styrene-d_8) (SBS) block copolymer subjected to shear flow. Evidence for the two structures includes in-situ SANS scattering patterns in which the two reflections relax independently after shearing[14] and direct observation of two distinct cylindrical packings in a sheared and quenched specimen by transmission electron microscopy (Figures 9–12) and SANS (Figure 5b).[27] The experimental observation of an additional cylindrical structure forming and coexisting with the original cylindrical morphology under shear is unique and coincides with some features of the model proposed earlier[14] and shown in Figure 1b (Model 2). The model is fundamentally changed, however, as illustrated in Figure 1c, because the $p3m1$ structure is expected to have no polystyrene center cylinder as the "center" spot (Figure 13b). Although this new morphology is a nonequilibrium structure, it is possible to quench in this structure under certain experimental conditions. For simplicity, we refer to the $p31m$ structure as "triangular hexagonal" and the $p3m1$ structure as "simple hexagonal".

The transformation of the $p31m$ unit cell of dimension $a = 25$ nm to a hexagonal microstructure of lower $p3m1$ symmetry, also with $a = 25$ nm, is analogous to martensitic transformations known in solid-state materials such as iron.[21,28] "Martensitic" is a general term used in metallurgy to describe shear-induced structural transformations of a particular nature. These transformations are defined as shear-dominant, lattice-distortive, diffusionless processes which occur by nucleation and growth.[21] The kinetics and morphology of the martensitic transitions are dominated by strain energy. In metals, these structures are also formed in deformation processes, and properties such as hardness are greatly improved.[34] The nature of our results on triblock copolymers is analogous to the molecular transformation which occurs in metals, but is on a mesoscopic scale. We use the term here to unite ideas and knowledge from two different types of materials which exhibit similar behavior.

The fact that the unit cell parameters for the two structures are actually the same ($a = 25$ nm) has important ramifications in this discussion. It is apparent from the symmetry of the two space groups shown in Figure 13 that only two structures with the same unit cell parameters will form, instead of structures with a wide range of apparent spacings. Similarly, the energy required for the transition to occur may not be very large, since the basic unit cell dimensions are unchanged. As outlined in Figure 13, the white PS cylinders at the positions marked 1, 2, and 3 remain stationary but reduce in size. Conservation of mass dictates the resultant cylinder size and polystyrene composition of the newly formed cylinders, shown as the shaded circles in Figure 13. It is important to note that the reduced cylinder diameter cannot be due to a simple elongation of the original triangular hexagonal structure, because of the lack of a central cylinder in the new structure and the alternating composition of the cylinders that are observed. Because of the preferred orientation of the original triangular hexagonal structure relative to the shear field (Figure 4b), imposition of a nonsymmetric deformation such as simple shear permits the transformation from the triangular hexagonal to the simple hexagonal structure. It is possible that if the triangular hexagonal structure had another orientation relative to the gradient direction, a different shear-induced morphology may be produced.

Although the identification of the two space groups allows us to gain understanding of this transformation purely on the basis of symmetry arguments, other theories to rationalize the molecular origin of the transformation have also been considered. A theoretical treatment of this transformation which considers the change in size and composition of the polystyrene cylinders would be an important addition to this work. However, the description of the effect of shear on the morphology of microphase-separated diblock copolymers provides a significant theoretical challenge. In triblock copolymers, the relative stability of the morphology is further complicated because of the presence of topological constraints, namely, loops and bridges. The response of these constraints to shear flow is difficult to predict. Even the simpler problem of diluted polymer solutions subject to shear is imperfectly understood because of the limited knowledge of the non-Newtonian properties of entangled polymer solutions.[35]

The most fundamental approach to this type of problem would follow the fluctuating hydrodynamics approach as applied by Onuki and Kawasaki[36] to ordinary small-molecule, near-critical, binary fluid mixtures subject to shear. A generalization of this approach to block copolymers would account for the different type of thermodynamic instability involved in block copolymer microphase separation and for the non-Newtonian flow properties of this kind of fluid. Alternatively, it seems appropriate to model such sheared complex fluids

phenomenologically by treating the steady state shear condition as a quasi-equilibrium state. This approach formally allows for a discussion of the observed morphological transition in terms of equilibrium theory which has the advantage that the transition in morphology can be discussed using chain molecular parameters. Such molecular details are often difficult to express in the more fundamental (but difficult to implement) fluctuating hydrodynamic approach. A discussion of the merit of the nonequilibrium versus the quasi-equilibrium point of view in describing the steady shear flow of phase-separating fluids is given elsewhere.[36,37]

From the quasi-equilibrium standpoint, the morphological transition in sheared systems occurs when sufficient energy has been input into the flowing copolymer to "excite" the copolymer into a higher free energy state. Such a state would be unstable under quiescent conditions. This phenomenology is somewhat analogous to the excitation of molecules to quantum states with radiation of the appropriate energy. Of course, the quantum analogy is imperfect because the excitation in the block copolymers occurs for *any* sufficiently high strain energy, while the quantum mechanical absorption occurs only at singular frequencies. However, this simple approach yields the important result that *only* two spacings are predicted, with no intermediate states, in agreement with our experimental observations.

Acknowledgment. The authors thank M. Muthukumar for originally proposing the existence of two kinds of morphological states in the presence of shear flow. We also gratefully acknowledge J. Douglas and R. Briber for helpful discussions throughout the course of this work. The possibility of a martensitic transformation in a triblock copolymer under shear was originally suggested by J. Cahn. We gratefully acknowledge his insight into this phenomenon. F.A.M. acknowledges the Petroleum Research Fund, administered by the American Chemical Society, and the National Science Foundation (Grant DMR 9111318) for partial support of this research.

References and Notes

(1) Bates, F. S.; Fredrickson, G. H. *Annu. Rev. Phys. Chem.* **1990**, *41*, 525.
(2) Brown, R. A.; Masters, A. J.; Price, C.; Yuan, X. F. In *Comprehensive Polymer Science*; Pergamon Press: Oxford, 1989; Vol. 2.
(3) Mayes, A. M.; Olvera de la Cruz, M. *J. Chem. Phys.* **1989**, *91*, 7228.
(4) Hamley, I. W.; Koppi, K. A.; Rosedale, J. H.; Bates, F. S.; Almdal, K.; Mortensen, K. *Macromolecules* **1993**, *26*, 5959.
(5) Bates, F. S.; Rosedale, J. H.; Fredrickson, G. H. *J. Chem. Phys.* **1990**, *92*, 6255.
(6) Koppi, K. A.; Tirrell, M.; Bates, F. S. *Phys. Rev. Lett.* **1993**, *70*, 1449.
(7) Winey, K. I.; Patel, S. S.; Larson, R. G.; Watanabe, H. *Macromolecules* **1993**, *26*, 2542.
(8) Albalak, R. J.; Thomas, E. L. *J. Polym. Sci., Polym. Phys. Ed.* **1993**, *31*, 37.
(9) Keller, A.; Pedemonte, E.; Willmouth, F. M. *Kolloid Z. Z. Polym.* **1970**, *238*, 385.
(10) Hadziioannou, G.; Mathis, A.; Skoulios, A. *Colloid Polym. Sci.* **1979**, *257*, 136.
(11) Morrison, F. A.; Winter, H. H.; Gronski, W.; Barnes, J. D. *Macromolecules* **1990**, *23*, 4200.
(12) Morrison, F. A.; Winter, H. H. *Macromolecules* **1989**, *22*, 3533.
(13) Winter, H. H.; Scott, D. B.; Gronski, W.; Okamoto, S.; Hashimoto, T. *Macromolecules* **1993**, *26*, 7236.
(14) Morrison, F.; Mays, J. W.; Muthukumar, M.; Nakatani, A. I.; Han, C. C. *Macromolecules* **1993**, *26*, 5271.
(15) Larson, R. G. *Rheol. Acta* **1992**, *31*, 497.
(16) Rangel-Nafaile, C.; Metzner, A. B.; Wissbrun, K. F. *Macromolecules* **1984**, *17*, 1187.
(17) Helfand, E.; Wasserman, Z. R. *Macromolecules* **1980**, *13*, 994–998. Helfand, E.; Wasserman, Z. R. *Developments in Block Copolymers*; Goodman, I., Ed.; Applied Science: New York, 1982. Fredrickson, G. H.; Helfand, E. *J. Chem. Phys.* **1987**, *87*, 697.
(18) Leibler, L. *Macromolecules* **1980**, *13*, 1602.
(19) Fredrickson, G. H. *J. Chem. Phys.* **1986**, *85* (9), 5306.
(20) Marques, C. M.; Cates, M. E. *J. Phys. Fr.* **1990**, *51*, 1733. Cates, M. E.; Milner, S. T. *Phys. Rev. Lett.* **1989**, *62*, 1856.
(21) Olson, G. B. In *Martensite*; ASM International: Metals Park, OH, 1992; Chapter 1.
(22) Certain commercial materials and equipment are identified in this paper in order to specify adequately the experimental procedure. In no case does such identification imply recommendation or endorsement by the National Institute of Standards and Technology nor does it imply that the material or equipment identified is necessarily the best available for this purpose.
(23) Nakatani, A. I.; Kim, H.; Han, C. C. *J. Res. Natl. Inst. Stand. Technol.* **1990**, 95, 7.
(24) Sakurai, S.; Sakamoto, J.; Shibayama, M.; Nomura, S. *Macromolecules* **1993**, *26*, 3351.
(25) Hashimoto, T.; Nagatoshi, K.; Todo, A.; Hasegawa, H.; Kawai, H. *Macromolecules* **1974**, *7*, 364.
(26) Odell, J. A.; Dlugosz, J.; Keller, A. *J. Polym. Sci., Polym. Phys. Ed.* **1976**, *14*, 861.
(27) Jackson, C. L.; Muthukumar, M.; Barnes, K. A.; Morrison, F. A.; Mays, J. W.; Nakatani, A. I.; Han, C. C. *Polym. Prepr. (Am. Chem. Soc., Div. Polym. Chem.)* **1994**, *35* (1), 624.
(28) *International Tables for Crystallography*; Hahn, T., Ed.; D. Reidel Publishing Co.: Amsterdam, 1983; Vol. A, pp 78–79.
(29) Handlin, D. L.; Thomas, E. L. *Macromolecules* **1983**, *16*, 1514.
(30) Dlugosz, J.; Keller, A.; Pedamonte, E. *Kolloid Z. Z. Polym.* **1970**, *242*, 1125.
(31) Roche, E. J.; Thomas, E. L. *Polymer* **1981**, *22*, 333.
(32) Hadziioannou, G.; Skoulios, A. *Macromolecules* **1982**, *15*, 267.
(33) Hashimoto, T.; Koizumi, S.; Hasegawa, H. *Macromolecules* **1994**, *27*, 1562.
(34) Waterstrat, R. M. *Platinum Met. Rev.* **1993**, *37* (4), 194.
(35) Douglas, J. F. *Macromolecules* **1992**, *25*, 1468.
(36) Onuki, A.; Yamazaki, K.; Kawasaki, K. *Ann. Phys.* **1981**, *131*, 217.
(37) Nakatani, A. I.; Douglas, J. F.; Ban, Y.-B.; Han, C. C. *J. Chem. Phys.* **1994**, *100*, 3224.

MA941116G